ISSN 1063-7826, Semiconductors, 2015, Vol. 49, No. 7, pp. 905–910. © Pleiades Publishing, Ltd., 2015.
Original Russian Text © D.S. Milakhin, T.V. Malin, V.G. Mansurov, Yu.G. Galitsin, K.S. Zhuravlev, 2015, published in Fizika i Tekhnika Poluprovodnikov, 2015, Vol. 49, No. 7, pp. 925–931.

Nitridation of an Unreconstructed and Reconstructed $(\sqrt{31} \times \sqrt{31})R \pm 9°$ (0001) Sapphire Surface in an Ammonia Flow

D. S. Milakhin[a]*, T. V. Malin[a], V. G. Mansurov[a], Yu. G. Galitsin[a], and K. S. Zhuravlev[a, b]**

[a] *Rzhanov Institute of Semiconductor Physics, Siberian Branch of the Russian Academy of Sciences, pr. Akad. Lavrent'eva 13, Novosibirsk, 630090 Russia*

[b] *Novosibirsk State University, ul. Pirogova 2, Novosibirsk, 630090 Russia*

*e-mail: *denironman@mail.ru, **zhur@thermo.isp.nsc.ru*

Submitted November 12, 2014; accepted for publication November 25, 2014

Abstract—This paper is devoted to the study of the nitridation of unreconstructed and reconstructed $(\sqrt{31} \times \sqrt{31})R \pm 9°$ (0001) sapphire surfaces in an ammonia flow by reflection high-energy electron diffraction (RHEED). The experimental results show that sapphire nitridation occurs on the unreconstructed (1 × 1) surface, which results in AlN phase formation on the substrate surface. However, if sapphire nitridation is preceded by high-temperature annealing (1150°C) resulting in sapphire surface reconstruction with formation of the $(\sqrt{31} \times \sqrt{31})R \pm 9°$ surface, the crystalline AlN phase on the sapphire surface is not formed during surface exposure to an ammonia flow.

DOI: 10.1134/S1063782615070180

1. INTRODUCTION

In connection with development of the optoelectronics industry, materials for the creation of highly reliable devices operating in a wide optical range are constantly being sought for [1]. Therefore, Group-III-nitride compounds are currently attracting more and more attention. Group-III nitrides are direct-gap semiconductors with various band gaps: 0.7 (InN), 3.4 (GaN), 6.2 (AlN) eV [2, 3]. AlGaN alloys span the near and far ultraviolet (UV) wavelength ranges; the use of InGaN-based compounds allows the development of light-emitting devices of the visible region. Therefore, Group-III nitrides are actively used in the development of light-emitting diodes, laser diodes, and UV photodetectors [4–6]. In addition to optoelectronic devices, Group-III nitride-based structures are also used in microwave electronics. Due to the pronounced polarity of Group III nitride compounds, spontaneous polarization, and the piezoelectric effect at the AlGaN/GaN heterojunction interface, a high concentration of two-dimensional electrons appears, which makes the structures with AlGaN/GaN heterojunction attractive for developing transistors. The high thermal stability and high breakdown fields make Group-III nitrides attractive in high-temperature and high-power electronics [7].

The most commonly used methods for fabricating GaN-based heterostructures are metal–organic chemical vapor deposition (MOCVD) and molecular-beam epitaxy (MBE), more precisely, ammonium MBE and MBE with nitrogen plasma activation. Since bulk GaN single-crystal production is a technologically complex and expensive process, a problem associated with the lack of native commercial substrates arises. Other substrates such as sapphire, Si, and SiC are used to form GaN epitaxial layers. The smallest lattice-parameter mismatch with GaN is inherent to SiC. A mismatch of ~3% and high thermal conductivity make SiC substrates very attractive for microwave and high-power electronics. However, a band gap comparable to that of GaN band excludes application of the substrate in the UV region, and the high cost limits application of the substrate in the commercial production of light-emitting devices of the visible region. Silicon substrates are promising due to the possibility of integrating nitride technology with developed silicon technology. However, the small band gap of Si leads to additional technological operations associated with the necessity of substrate removal in the case of optical applications, and the significant differences in lattice parameters and thermal expansion coefficients cause a number of difficulties in the fabrication of high-quality films. Sapphire substrates are transparent in the UV and visible regions, thermally stable, and possess sufficiently high thermal conductivity. Therefore, sapphire is the most commonly used substrate for growing Group-III nitride-based heterostructures for optoelectronic devices and transistors.

To match the parameters of Group-III nitride and sapphire lattices to the Al_2O_3 surface, a thin crystalline AlN layer is formed. The initial crystalline AlN phase on the Al_2O_3 substrate is usually formed by exposing the heated substrate to an active nitrogen flow. This

process referred to as "nitridation" depends on the form and flow of active nitrogen and the substrate temperature [1, 3, 8–14]. During nitridation, an AlN phase with AlN-cell rotation by 30° with respect to the Al_2O_3 cell is formed on the sapphire surface, which finally results in an effective lattice-parameter mismatch of 13%. The Al_2O_3 surface is reconstructed upon heating to 1000–1200°C, and the $(\sqrt{31} \times \sqrt{31})R \pm 9°$ reconstruction appears [15, 16]. The reconstruction is characterized by the formation of structures on clean single-crystal surfaces, whose unit cell has a period different from that in the crystal bulk (in planes parallel to the surface) and usually exceeding it by several times [17]. Agnarsson et al. [1] assert that the AlN phase is not formed at all on the unreconstructed Al_2O_3 surface, whereas nitridation occurs efficiently on the surface with the $(\sqrt{31} \times \sqrt{31})R \pm 9°$ superstructure. The mechanism of this phenomenon was not conclusively identified. The $(\sqrt{31} \times \sqrt{31})R \pm 9°$ reconstruction was studied in a number of works by atomic-resolution atomic-force microscopy and small-angle X-ray diffraction [18–23]. Models of the reconstructed surface were proposed based on the fact that the sapphire surface is enriched with metal aluminum at high temperatures. For example, it is argued that two additional Al planes are formed on the surface due to the decomposition of two surface layers and oxygen desorption, whose structure is close to the (111) planes of the cubic aluminum single crystal [18–20, 23]. In this case, it is reasonable to expect that the reconstruction promotes nitridation due to the high chemical activity of metal aluminum; however, studies of the effect of the reconstruction on nitridation are very small in number. Furthermore, despite the large number of publications describing the study of nitridation by various methods, there are still contradictory data on methods of the pre-epitaxial preparation of sapphire substrates and nitridation conditions. Therefore, the objective of this work is to study the mechanism of the interaction of ammonia with reconstructed and unreconstructed sapphire surfaces.

2. EXPERIMENTAL

Experiments for studying nitridation were carried out using a Riber CBE-32N(P) MBE setup equipped with a gaseous ammonia source. The experiments were performed using "epi-ready" (0001) sapphire substrates 50 mm in diameter. A molybdenum layer was deposited onto the rearside of the substrates, since the samples were heated during MBE by thermal radiation from a heater, which was a tantalum spiral placed into a pyrolytic boron-nitride mould. The substrates were preliminarily cleaned by annealing in a loading chamber at a temperature of 900°C in the residual atmosphere at a pressure of $(2–5) \times 10^{-8}$ Torr. The surface temperature was measured using an Ircon pyrometer (single-color intensity pyrometer). As the nitrogen source, ultra-pure grade 99.999 ammonia was used. Ammonia was fed to the chamber using automatically controlled pneumatic valves. The NH_3 flow rate to the growth chamber was set using a BronkHorst regulator in the range of 0–400 sccm.

Information about Al_2O_3 surface reconstruction and sapphire nitridation was obtained in situ using reflection high-energy electron diffraction (RHEED) with an electron energy of 11 keV. The electrons were incident on the surface at a grazing angle of ~(1–3)°. After interaction with the crystal, electrons in the form of diffraction beams arrived at a luminescent screen. The diffraction pattern displayed on the luminescent screen was recorded by a chamber representing a charge coupled device (CCD camera). Diffraction-pattern variation and reflection-intensity redistribution on the unreconstructed and reconstructed Al_2O_3 surfaces were observed during the experiment. Since sapphire is an insulator with a band gap of $E_g \times 9.5$ eV, charge is accumulated on the surface upon exposure to the electron beam (when using the RHEED method), which affects the quality of the measured experimental data. To decrease the effect of charging, the study was performed on samples with a thin molybdenum layer 0.15 μm deposited onto the front side of the (0001) sapphire substrate, except for a region in the center 4.5 mm in diameter (Fig. 1). The deposition of metal onto the substrate surface caused a charge decrease on the sapphire area under study.

The sapphire surface was analyzed before and after substrate exposure to ammonia. The first part of the experiment consisted in comparison of the diffraction patterns with the aim of revealing the crystalline AlN phase after substrate exposure to ammonia. To obtain the reconstructed surface $(\sqrt{31} \times \sqrt{31})R \pm 9°$, the samples were heated to 1150°C. The unreconstructed and reconstructed surfaces were exposed to an ammonia flow rate of 25 sccm for 30 min at a temperature of 840°C. The second part of the experiment consisted in filming by the CCD camera from the luminescent screen under conditions of continuous and steady rotation of the substrate. Such rotation makes it possible to observe many reflections under various nonequivalent diffraction conditions, to detect the possible redistribution of their intensities, and in general to reveal a larger number of changes in the diffraction patterns which may occur during sapphire-surface nitridation. The films with diffraction patterns were processed by measuring the intensity for certain stationary small image areas (e.g., 10 × 10 pixels), while the complete diffraction pattern continuously varies during rotation. Fixed areas were chosen so that the diffraction reflection of interest to fall would fall within a chosen area at certain azimuthal positions. The initial film frames were chosen so that the diffraction patterns would correspond to identical azimuthal positions of the samples.

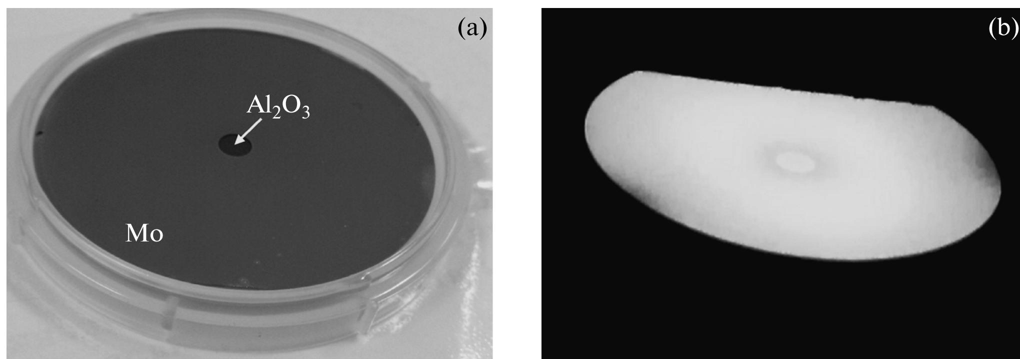

Fig. 1. (a) (0001) sapphire substrate with a molybdenum layer 0.15 μm thick deposited onto the front side, except for the central area 4.5 mm in diameter and (b) its view in a heated state.

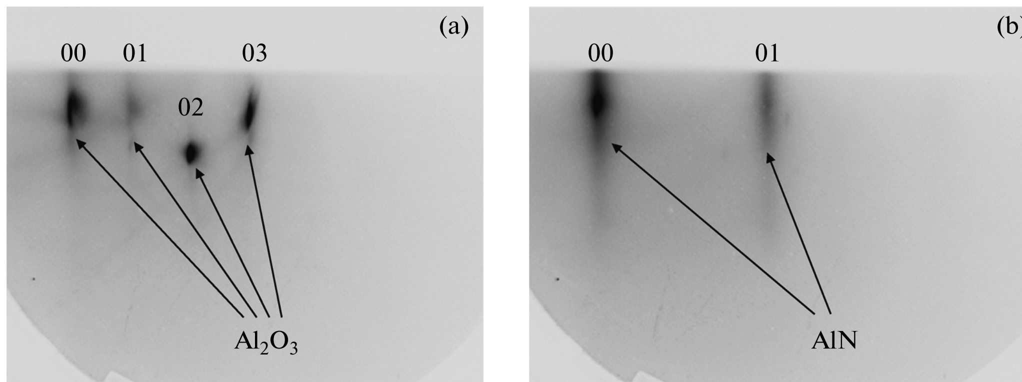

Fig. 2. Diffraction patterns with (a) sapphire reflections before nitridation and (b) nitride phase reflections after nitridation.

3. EXPERIMENTAL RESULTS

Figure 2 shows the diffraction patterns with reflections from the unreconstructed sapphire surface (a) before and (b) after nitridation at identical azimuthal positions. When comparing these images, it can be noted that the 01 and 02 reflections of unreconstructed sapphire after nitridation almost completely vanished, and the 01 reflection of crystalline aluminum nitride appeared near the 03 reflection.

Experimental data about the AlN and Al_2O_3 reflection intensity, obtained by processing the 01 AlN and 02 Al_2O_3 reflections, i.e., an increasing time dependence of the aluminum-nitride reflection intensity and the sloping time dependence of the sapphire reflection intensity at a constant nitridation temperature of 840°C and an ammonia flow rate of 25 sccm, are shown in Fig. 3.

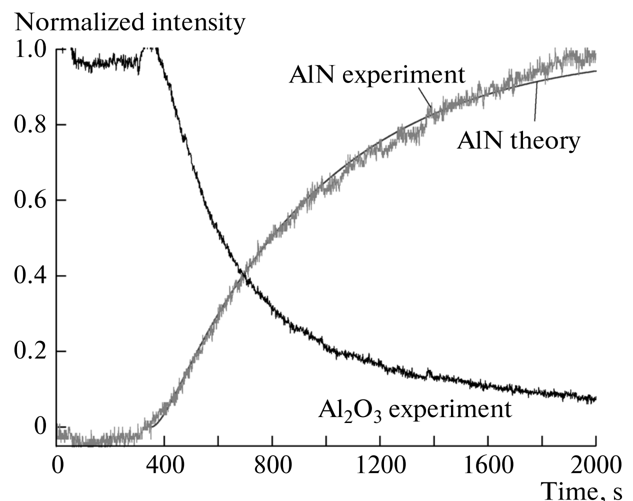

Fig. 3. Experimental and calculated time dependences of the reflection intensity of aluminum nitride and sapphire at a constant temperature of 840°C in an ammonia flow rate of 25 sccm.

To explain the phenomena of the nitridation of the unreconstructed sapphire surface, the following schematic of processes on the substrate surface was proposed (Fig. 4): during heating of the Al_2O_3 substrate, aluminum on the surface is partially reduced to AlO [15]; the dissociative chemisorption of NH_3 occurs during nitridation. Adsorbed radicals recombine at the surface with the formation of nitrogen and hydrogen molecules. The formed nitrogen molecules with very strong interatomic bonds cannot interact with aluminum at such low temperatures (840°C). Simulta-

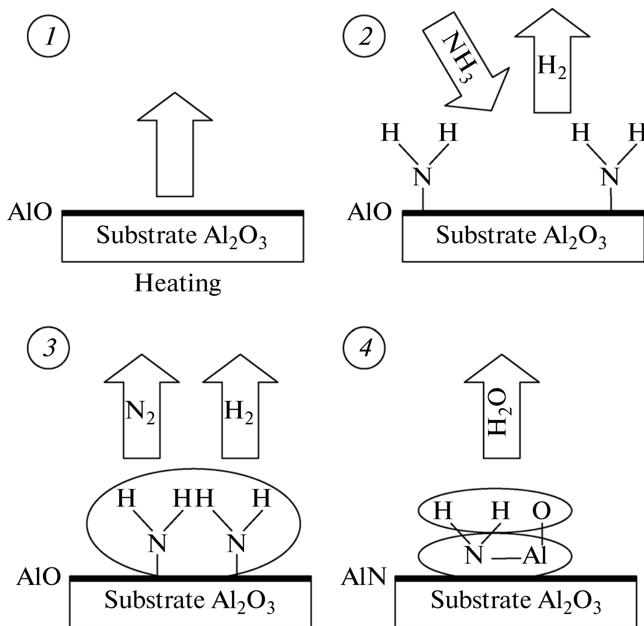

Fig. 4. Schematic diagram of nitridation of an unreconstructed sapphire surface: (*1–4*) sequence of reactions.

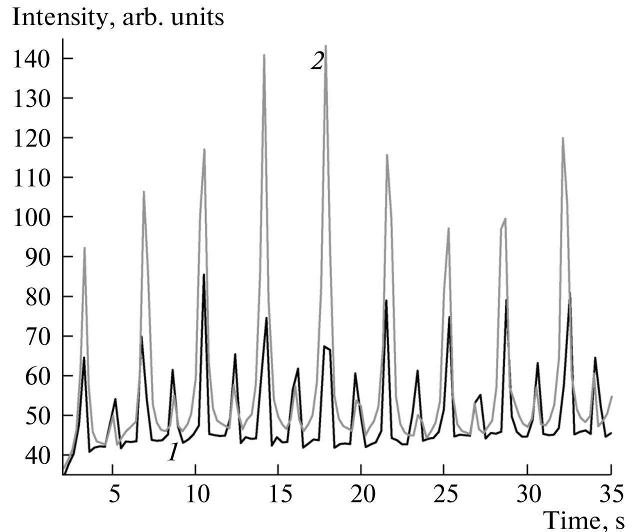

Fig. 5. Comparison of reflection intensities of an unreconstructed (0001) sapphire surface (*1*) before and (*2*) after nitridation.

neously with radical recombination, the crystalline phase of aluminum nitride is formed.

We described the scheme for the surface concentrations usingby means of differential equations: the first equation describes the variation in the adsorbed ammonia (NH_2^{ads}) concentration on the surface for the time t; P is the ammonia pressure; the second equation describes the variation in the reduced aluminum AlO concentration on the surface, the minus sign indicates a decrease in the AlO concentration on the surfaces with time; the last equation describes the AlN-phase accumulation rate. Each reaction occurs with a certain probability defined by the kinetic constants k_1, k_2, k_3,

$$d\left[\frac{NH_2^{ads}}{dt}\right] = k_1P(1-[NH_2^{ads}]) - k_2[NH_2^{ads}]^2 - k_3[NH_2^{ads}]\cdot[AlO], \quad (1)$$

Reaction constants as a function of the chemical reaction type

Chemical reaction	Activation energy E_{act}, eV	Pre-exponential factor k_0, 1/s
Dissociative chemisorption of NH_3	−1.5	6×10^4
Recombination of NH_2 radicals	−4.0	3×10^{13}
AlN phase formation	−5.3	7×10^{19}

$$\frac{d[AlO]}{dt} = -k_3[NH_2^{ads}]\cdot[AlO], \quad (2)$$

$$\frac{d[AlN]}{dt} = k_3[NH_2^{ads}]\cdot[AlO]. \quad (3)$$

These differential equations were solved numerically with the result that the reaction constants were determined, i.e., the activation energy E_{act}, in other words, the minimum energy required to be imparted to the system to initiate the reaction, and the pre-exponential factor k_0 characterizing the particle collision frequency (see table). The temperature T is constant, $T = 910°C$, k_B is the Boltzmann constant,

$$k_i = k_0e^{-E_{act}/k_BT}, \quad i = 1, 2, 3. \quad (4)$$

At these kinetic constants, the calculated curves of the aluminum-nitride and ammonia intensities were constructed (Fig. 3). The coincidence of the experimental and calculated AlN curves points to the accuracy of the kinetic constants and the plausibility of the kinetic scheme.

The reflection intensity was measured in the second part of the experiment, as noted above, in certain stationary areas of the diffraction pattern. The AlN and sapphire reflection intensities at various azimuths passed through these areas during sample rotation. Figure 5 shows the oscillatory dependences of the reflection intensities of the unreconstructed sapphire surface before and after exposure to ammonia. The initial portions of the intensity measurements were chosen in the $[1\bar{1}00]$ directions. An increase in the peak intensity after nitridation is associated with the formation of AlN reflections near sapphire reflections,

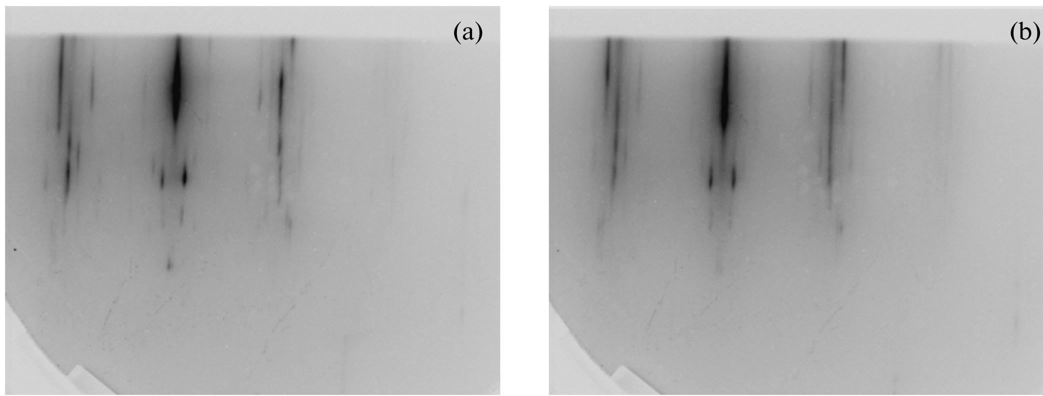

Fig. 6. Reconstructed ($\sqrt{31} \times \sqrt{31}$)$R \times 9°$ (0001) sapphire surface (a) before and (b) after exposure to ammonia.

which confirms formation of the crystalline AlN phase on sapphire. Figure 6 shows the diffraction pattern of the reconstructed ($\sqrt{31} \times \sqrt{31}$)$R \pm 9°$ (0001) sapphire surface obtained by high-temperature annealing (1150°C) (a) before and (b) after exposure to ammonia. We can see that the diffraction pattern of the sapphire surface after exposure to ammonia differs in no way from the initial one, which indicates the absence of newly formed crystalline phases.

We can see from oscillations shown in Fig. 7 that exposure to ammonia did not cause any reflection-intensity redistribution; hence, no new crystalline phase on the reconstructed sapphire surface was formed.

These results contradict the data obtained in [1], where the effect of the initial surface reconstruction on (0001) sapphire-surface nitridation was studied using low-pressure ammonia. To analyze the surface, Agnarsson et al. [1] used reflection low-energy electron diffraction (RLEED) and electron spectroscopy for chemical analysis (ESCA). Chemical analysis of the surface confirmed the presence of Al–N bonds. As the experiments [1] showed, a peak corresponding to the Al–N chemical bond with a higher amplitude was observed on the substrate with the reconstructed surface. However, analysis of the diffraction patterns obtained by the RLEED method [1] did not detect an AlN crystalline phase on the reconstructed sapphire surface. Thus, the exposure of reconstructed sapphire to ammonia results in the formation of chemical bonds, but atomic ordering does not occur in this case, since both RHEED and RLEED do not detect AlN reflections on the diffraction patterns. In the case of definition of the concept of nitridation as the formation of the crystalline AlN phase exactly during exposure of the heated substrate to an ammonia flow, it can be argued that nitridation occurs efficiently on the unreconstructed surface.

Despite the expectation of higher chemical activity of the reconstructed ($\sqrt{31} \times \sqrt{31}$)$R \times 9°$ (0001) sapphire surface (in comparison with the unreconstructed surface), the nitridation process was not activated in the case at hand due to surface enrichment with metal aluminum according to the proposed models [18–20, 22, 23]. In [18], the chemical passivity of this reconstructed surface and its stability against atmospheric oxygen at room temperature were also indicated, which the authors attempted to explain by the presence of kinetic limitations. However, it was shown in [24] that clean Al (111) surface oxidation begins at an exposure dose of ~60 L (the dose of 1 Langmuir corresponds to the number of particles which collided with the surface at a pressure of 10^{-6} Torr in 1 s), and the surface is completely covered with oxygen at a dose of ~1300 L. Certainly, the exposure dose of atmospheric oxygen is higher by several orders of magnitude, and the oxidation of metal aluminum should occur. The revealed contradiction probably suggests that alumi-

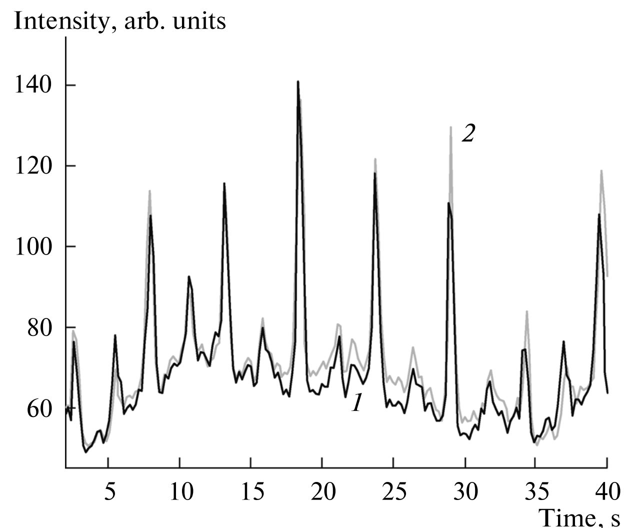

Fig. 7. Comparison of reflection intensities of the reconstructed ($\sqrt{31} \times \sqrt{31}$)$R \times 9°$ (0001) sapphire surface (*1*) before and (*2*) after nitridation.

num is not completely reduced to the metal state, but only partial reduction occurs, as expected in [15].

The stability of reconstructed sapphire to ammonia processing can be explained assuming that nitridation is a typical topochemical reaction. As is known, such reactions are characterized by new phase nucleation on lattice surface defects followed by nuclei growth. Since surface reconstruction results from high-temperature exposure to the surface, it can be assumed that the number of primary-AlN formation nuclei in the case of reconstruction will become much smaller than on the unreconstructed sapphire surface. Thus, the nitridation process is inhibited so much that obtaining the crystalline AlN phase on the surface of reconstructed sapphire under MBE conditions seems complicated.

4. CONCLUSIONS

The present experiments show that efficient nitridation of the (0001) sapphire surface under MBE conditions requires an unreconstructed surface. To describe the nitridation mechanism of the unreconstructed (0001) sapphire surface, a kinetic scheme of the nitridation process was proposed. The studies showed that the exposure of the reconstructed ($\sqrt{31} \times \sqrt{31}$)$R \times 9°$ surface does not lead to crystalline AlN phase formation, from which it follows that the reconstructed surface is more stable to the exposure to ammonia.

ACKNOWLEDGMENTS

This study was supported by the Russian Foundation for Basic Research (projects nos. 13-02-00985, 14-02-00033, 14-02-92007, 14-02-91371) and the Ministry of Education and Science of the Russian Federation (agreement no. 14.578.21.0062).

REFERENCES

1. B. Agnarsson, M. Göthelid, S. Olafsson, H. P. Gislason, and U. O. Karlsson, J. Appl. Phys. **101**, 013519 (2007).
2. S. Strite and H. Morkoc, J. Vac. Sci. Technol. B **10**, 1237 (1992).
3. K. Uchida, A. Watanabe, F. Yano, M. Kouguchi, T. Tanaka, and S. Minagawa, J. Appl. Phys. **79**, 3487 (1996).
4. S. Nakamura, T. Mukai, and M. Senoh, Jpn. J. Appl. Phys., pt. 2 **30**, L1708 (1991).
5. Y. Cho, Y. Kim, E. R. Weber, S. Ruvimov, and Z. Liliental-Weber, J. Appl. Phys. **85**, 7909 (1999).
6. Y. Saito, T. Akiyama, K. Nakamura, and T. Ito, J. Cryst. Growth **362**, 29 (2013).
7. A. N. Alexeev, D. M. Krasovitskii, S. I. Petrov, and V. P. Chaly, Semiconductors **46**, 1429 (2012).
8. T. Yamaguchi, T. Araki, Y. Saito, K. Kano, H. Kanazawa, Y. Nanishi, N. Teraguchi, and A. Suzuki, J. Cryst. Growth **237–239**, 993 (2002).
9. K. Balakrishnan, H. Okumura, and S. Yoshida, J. Cryst. Growth **189–190**, 244 (1998).
10. F. Widmann, G. Feuillet, and J. L. Rouvière, J. Appl. Phys. **85**, 1550 (1999).
11. G. Namkoong, W. A. Doolittle, and A. S. Brown, J. Appl. Phys. **91**, 2499 (2002).
12. C. Heinlein, J. K. Grepstad, S. Einfeldt, D. Hommel, T. Berge, and A. P. Grande, J. Appl. Phys. **83**, 6023 (1998).
13. N. Grandjean, J. Massies, and M. Leroux, J. Appl. Phys. **69**, 2071 (1996).
14. Y. Wang, S. A. Özcan, G. Özaydin, K. Ludwig, Jr., A. Bhattacharyya, T. D. Moustakas, H. Zhou, R. L. Headrick, and D. P. Siddons, Phys. Rev. B **74**, 235304 (2006).
15. T. M. French and G. A. Somorjai, J. Phys. Chem. **74**, 2489 (1970).
16. P. S. P. Wei and A. W. Smith, J. Vac. Sci. Technol. **9**, 1209 (1972).
17. Physical Encyclopedy. http://dic.academic.ru/dic.nsf/enc_physics/4526 /REKONSTRUKTsIYa
18. G. Renaud, B. Villette, I. Vilfan, and A. Bourret, Phys. Rev. Lett. **73**, 1825 (1994).
19. A. Chame, F. Lancon, P. Politi, G. Renaud, I. Vilfan, and J. Villain, Int. J. Mod. Phys. B **11**, 3657 (1997).
20. I. Vilfan, F. Lancon, and J. Villain, Surf. Sci. **392**, 62 (1997).
21. C. Barth and M. Reichling, Nature **414**, 54 (2001).
22. E. A. A. Jarvis and E. A. Carter, J. Phys. Chem. B **105**, 4045 (2001).
23. J. V. Lauritsen, M. C. R. Jensen, K. Venkataramani, B. Hinnemann, S. Helveg, B. S. Clausen, and F. Besenbacher, Phys. Rev. Lett. **103**, 76103 (2009).
24. H. Brune, J. Wintterlin, J. Trost, G. Ertl, J. Wiechers, and R. J. Behm, J. Chem. Phys. **99**, 2128 (1993).

Translated by A. Kazantsev